Perovskite-Based Artificial Vision System for In-Sensor Image Processing

Shivam Kumar[1], Swapnadeep Poddar[1], Zhenghao Long[1], Zhiyong Fan[1]
[1] Dept. of ECE, The Hong Kong University of Science and Technology, Clear Water Bay, Hong Kong

Abstract
Inspired by the human visual system, we present a perovskite nanowire-based artificial vision system (AVS) with potential for in-sensor image processing. The AVS exhibits a consistent response to various optical stimuli and displays characteristics such as learning and forgetting. We fabricate a 10-by-10 crossbar array device to demonstrate contrast enhancement capabilities and integrate it with perovskite-based memory for recognizing different geometric shapes.

Keywords
Perovskite, Vision system, Biomimetics

Introduction
Vision is the most important sensory modality for humans, accounting for approximately 80% of the information we perceive [1]. Efforts to replicate the functionality of the human eye have led to the development of contemporary charge-coupled device (CCD) and complementary metal-oxide-semiconductor (CMOS) image sensors. However, these artificial sensors often fall short of their biological counterparts in several performance metrics [2]. Traditional frame-based image sensors necessitate the use of an image processing unit, resulting in significant computational demands on modern central processing units (CPUs). In contrast, the human retina undertakes fundamental preprocessing tasks, such as contrast enhancement and edge detection, prior to transmitting information to the visual cortex for further processing [3]. This intrinsic preprocessing capability significantly reduces the cognitive load on the brain and improves energy efficiency. Such a vision system is particularly beneficial for computer vision applications, including those implemented in autonomous robotic systems [4].

Inspired by the human retina, we present an artificial vision system(AVS) composed of a vertically aligned all-inorganic perovskite nanowire array embedded within a porous aluminum oxide membrane (PAM). The lead hallide perovskite ($MAPbBr_3$) device exhibits exceptional stability, with the aluminum oxide membrane offering protection against moisture and preventing degradation [5]. The AVS is capable of operating in both frame-based imaging mode and neuromorphic mode, attributed to its unique band alignment [6]. We demonstrate various imaging and basic processing tasks, such as contrast enhancement and learning and forgetting, using a 10 by 10 crossbar array device. Additionally, we integrate a 6 by 6 photonic synapse device array with a perovskite-based resistive random-access memory (R-RAM) array for the recognition of different geometric shapes. The device also has the potential to be configured in a hemispherical shape, structurally mimicking the human retina, which offers advantages such as an expanded field of view, simplified optics, and reduced optical aberration [7].

Device Fabrication and Characterization
Fig. 1A illustrates the schematic of the biological visual system. In this system, photoreceptor cells in retina convert photons into electrical impulses, which are subsequently pre-processed by bipolar and ganglion cells. This layer performs essential functions such as contrast enhancement, edge detection, and motion detection before transmitting the signals through the optic nerve to the visual cortex for final processing. In a manner analogous to the structure of photoreceptive cells, the Artificial Vision System (AVS) consists of vertically aligned perovskite nanowires within an anodized aluminum oxide (AAO) membrane, as depicted in Fig. 1B. The AAO membrane is produced through a two-step anodization process of electrochemically polished aluminum chips [8]. Lead (Pb) nanowires are then deposited into the nanochannels via an electro-deposition technique. A thin layer of tin oxide (SnO2), serving as the electron transport layer, is conformally deposited along the side walls of the AAO membrane using atomic layer deposition. The perovskite nanowires are subsequently grown through a chemical vapor deposition process. Top and bottom crossbar indium tin oxide (ITO) electrodes are deposited using radio frequency (RF) sputtering with a shadow mask. The entire system is encapsulated with UV epoxy on a printed circuit board (PCB). The perovskite device can perform absorption and preprocessing of the incident image, which can then be utilized by another resistive random-access memory (R-RAM) layer for geometric shape detection.

To gain a comprehensive understanding of the device's operational mechanism, we utilize the band diagram representing the entire metal (Pb) – semiconductor (MAPbBr3) – electron transport layer (ETL) (SnO2) – metal (ITO) interfaces, as shown in Fig. 2A. The unique behavior of the device arises from the charge trapping and de-trapping dynamics at the perovskite–Pb interface. When a small voltage of 0.01 V is applied across the electrodes, the device operates in standard imaging mode, leading to the formation of a minor Schottky junction at the metal–semiconductor contact. Upon photon absorption by the semiconductor, the generated holes become trapped at this Schottky junction. As more holes accumulate at this interface, the semiconductor transitions to a heavily p-doped state, which lowers its energy bands and alters the formation of the Schottky contact. Conversely, when a significant bias is applied across the electrodes, the band bending at the Schottky contact increases. This enhanced band bending allows for a greater number of photo-generated holes to be trapped within the semiconductor, thereby increasing its conductivity. This gradual enhancement in conductivity ultimately leads to the neuromorphic behavior exhibited by the device.

ISSN 0097-996X/25/5601-0381-$1.00 © 2025

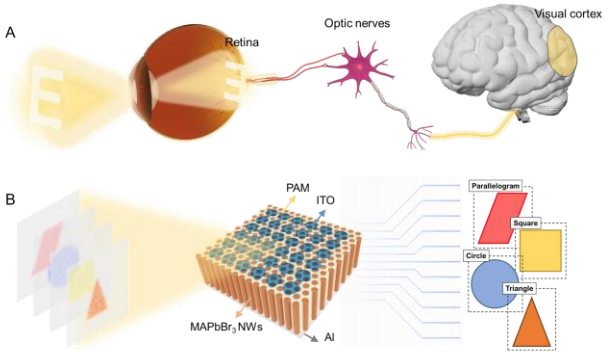

Fig 1: (A) Schematic showing the human visual system with data captured and pre-processed by the retina, relayed by the optic nerves and processed by the visual cortex. (B) Schematic showing the artificial visual system (AVS) showing the image captured and pre-processed by the perovskite image sensor and further relayed for shape classification.

Fig. 2B presents an actual photograph of a flexible device fabricated on a flexible PET substrate, resembling its biological counterpart. The scanning electron microscopy (SEM) image of the nanostructures is depicted in Fig. 2C, where the vertical nanowires within the anodic aluminum oxide (AAO) membrane emulate the photoreceptor cells found in the retina. The chemical vapor deposition (CVD) process employed for semiconductor growth results in a remarkably high filling ratio within the nanochannels, as illustrated in Fig. 4D. Additionally, we investigated the crystal properties of the perovskite using transmission electron microscopy (TEM), revealing that our process produces single crystalline nanowires with different growth orientations, as shown in Fig. 2E-F.

Fig. 3A and Fig. 3D present the photoluminescence (PL) and X-ray diffraction (XRD) spectra of the nanowire MAPbBr3 device. Notably, the passivating properties of the anodized aluminum oxide (AAO) membrane enhance the longevity of the device, as evidenced by the retention of PL spectra and XRD characteristics even after one week of storage in high humidity conditions. This distinctive behavior contrasts with that of thin-film counterparts and is attributed to the insulating properties of the membrane.

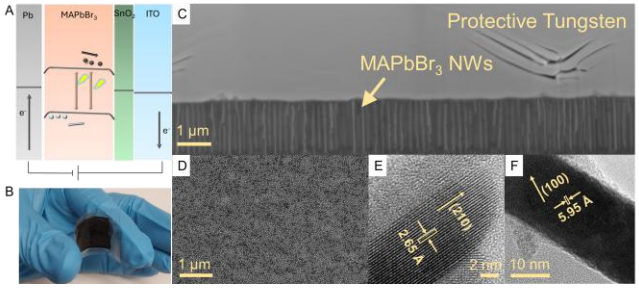

Fig 2: (A) Band diagram and working principle of the AVS. (B) Optical image of a curved AVS. (C) SEM image of the device showing perovskite inside the AAO channel. (D) Top view SEM image of the device showing high filling ratio. (E-F) TEM image of the perovskite nanowire showing high crystallinity.

Fig. 3B illustrates the potentiation and depression observed in the artificial vision system (AVS) in response to varying light intensities. The data indicate that conductance increases with higher incident light intensity on the AVS. A similar trend is noted with prolonged illumination time, as depicted in Fig. 3C. Fig. 3E demonstrates the change in current resulting from two light pulses separated by a time interval of $\Delta t = 2$ seconds, resembling the response of a neuron to presynaptic and postsynaptic pulses. Fig. 3F displays the optical paired pulse facilitation (PPF) response, indicating that the response diminishes as the time difference between the incident light pulses increases. The PPF measurement validates the short-term plasticity exhibited by the AVS, which is essential for neuromorphic behavior. Notably, the packaged device continued to perform effectively even after six months of use, further corroborating the beneficial impact of the AAO passivation.

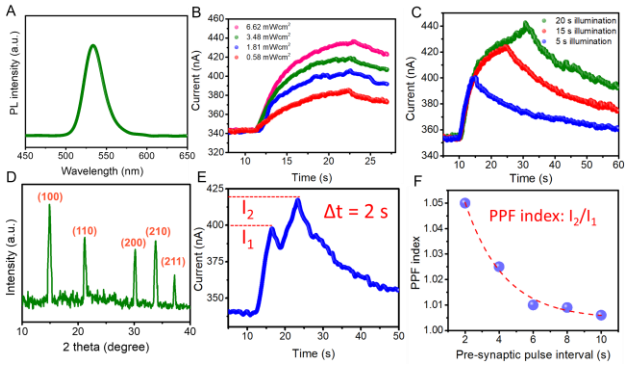

Fig 3: (A) PL spectra of the perovskite nanowire in AAO template. (B) Current vs time data showing the potentiation and depression of the AVS device for different light intensity. (C) Current vs time data showing the potentiation and depression of the AVS device for different illumination time. (D) XRD spectra of the perovskite material grown in the AAO template. (E) Current response of AVS to pre-synaptic and post-synaptic light with $\Delta t = 2$ s. (F) PPF with Δt varying between 2 and 10 s.

Shape Classification

We demonstrate the imaging and computational capabilities of the device utilizing a 10 by 10 crossbar array. Fig. 4A presents the schematic of the crossbar array device. Measurements were conducted using a NI 2530B multiplexer and a Keithley 2450 source measure unit (SMU) synchronized using a python program, as illustrated in Fig. 4B. A simple image was input into the AVS, as shown in Fig. 4C, with the resultant image captured by the standard device depicted in Fig. 4D. As illustrated in Fig. 4E(i)–(iii), continuous projection of the image onto the AVS results in a gradual increase in current, which enhances the brightness of the captured image, resembling the learning process observed in humans. Conversely, upon removal of the image (Fig. 4E(iv)–(vi)), the phenomenon of forgetting occurs, leading to a gradual decay in current.

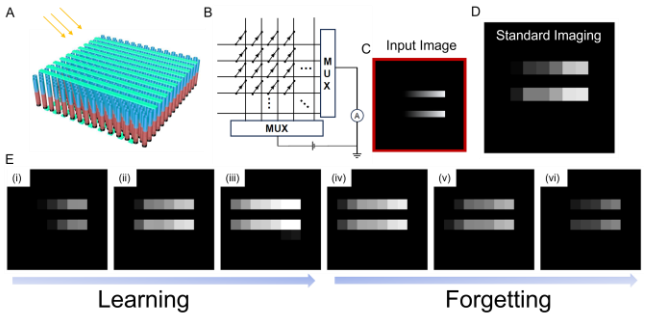

Fig 4: (A) Schematic of a 10 by 10 cross bar array. (B) Schematic of the current readout circuit. (C) Image input on the AVS (D) Standard imaging obtained by the AVS (E) Learning and Forgetting information obtained by the AVS

To further explore the advantages of the artificial vision system, we integrate the output of a 6 by 6 neuromorphic device array with a 36 by 4 electronic synapse array. This electronic synapse array is constructed using a perovskite resistive random-access memory (R-RAM) crossbar structure [9]. The weights for the R-RAM layer are initially determined through online training and subsequently assigned to the R-RAM cells based on their resistance values. The array receives 36 inputs from the image sensor layer and generates 4 outputs, which are computed using the nonlinear activation function described in Equation (1).

$$output = \sum_{i=0}^{36}(pixel_i * weight) \qquad (1)$$

The electronic synapse array consists of 36 rows and 4 columns. The total current from each column represents the output corresponding to a specific shape (triangle, square, circle, and parallelogram). The outputs from the 4 columns are normalized to determine the recognition probabilities for the four shapes. In summary, the system features 36 outputs in the perception layer (6 by 6 array), 36 rows in the input layer, and 4 rows in the output layer (36 by 4 array).

Fig. 5A illustrates the varying weights assigned to the 36 by 4 R-RAM array and their evolution over a time span from 10 seconds to 10^5 seconds. We observed minimal significant changes in the resistance values over time, highlighting the robust nature of the nanowire R-RAM device.

Different geometric shapes, accompanied by randomly generated noise, were projected onto the AVS, as shown in Fig. 5B(i). The device effectively mitigated the noise, demonstrating its neuromorphic behavior (Fig. 5B(ii)). Fig. 5C presents the recognition probabilities for various shapes projected onto the AVS over an extended duration. The recognition probabilities consistently exceeded 99%, with false positives and false negatives remaining below 1% for all four shapes.

Furthermore, we noted that recognition accuracy improves with increased incident light intensity of the geometric shapes, attributed to the accelerated learning process that occurs at higher light levels. Noisy images were projected onto both the AVS device and an event-based image sensor (without photonic synapse) prior to being input into the electronic synapse. Our results indicate that the training loss in the AVS device converges significantly faster (Fig. 5E), achieving 100% accuracy after just 66 training epochs, compared to the 2348 epochs required by the event-based sensor system. A similar trend was observed in recognition accuracy, with the AVS reaching over 99% accuracy after only 66 epochs, while the event-based sensor required more than 2000 epochs to achieve comparable performance.

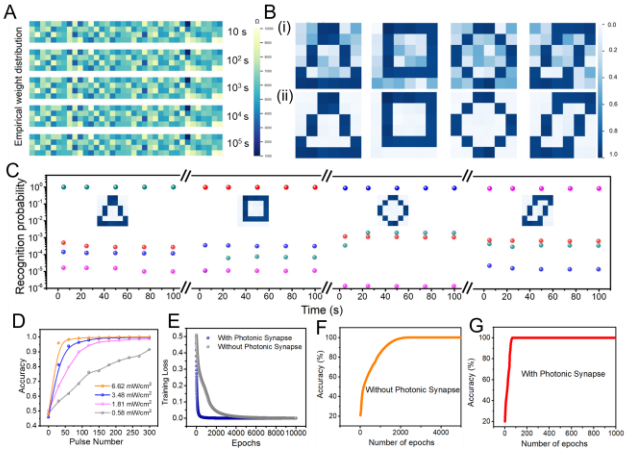

Fig 5: (A) Evolution of weight distribution in the R-RAM array for different shapes over time. (B) Plot showing the classification result with and without randomly generated noise. (C) Recognition probabilities of different shapes. (D) Accuracy of shape recognition against different pulse number and incident light intensity. (E) Effect of photonic synapse (AVS) on the training loss plotted against epochs. (F) The accuracy vs epochs for the system without AVS. (G) The accuracy vs epochs for the system with AVS.

Conclusion

In this study, we introduce a human retina-inspired artificial vision sensor constructed from a high-density, vertically aligned array of perovskite nanowires. This all-inorganic device demonstrates exceptional stability in photo response, maintaining 90% of its performance after 14 months of operation. Notably, the device exhibits synaptic responses at elevated applied biases, facilitating data preprocessing and alleviating computational demands on the image processor. We have fabricated a 10 by 10 crossbar array of this device, which consistently responds to various optical signals, simulating learning and forgetting processes. Furthermore, we explore the full capabilities of the artificial vision system by integrating a perovskite nanowire-based photonic synapse array with a perovskite nanowire-based resistive random-access memory (R-RAM) array, employing it for geometric shape classification tasks. This integration achieves an impressive accuracy of 99%, significantly surpassing that of an event-based image sensor in a comparable setup and requiring fewer training epochs. This research paves the way for the development of more advanced and efficient artificial vision systems.

Acknowledgments

The authors would like to thank Mr. Peter Nam and Mr. Jacob Ho from the dept. of ECE, HKUST for assistance in purchasing and setting up the equipment used in the experiments.

References

[1] F. Hutmacher, “Why Is There so Much More Research on Vision than on Any Other Sensory Modality?”, Frontiers in Psychology, vol. 10, no. 2246, Oct. 2019.

[2] J. Zhang, S. Dai, Y. Zhao, J. Zhang, and J. Huang, “Recent Progress in Photonic Synapses for Neuromorphic Systems”, Advanced Intelligent Systems, vol. 2, no. 3, p. 1900136, Jan. 2020.

[3] G. D. Hildebrand and A. R. Fielder, “Anatomy and Physiology of the Retina”, Pediatric Retina, pp. 39–65, Aug. 2010.

[4] S. Poddar et al., “Geometric Shape Recognition with an Ultra-High Density Perovskite Nanowire Array-Based Artificial Vision System”, ACS Applied Materials & Interfaces, vol. 16, no. 4, pp. 5028–5035, Jan. 2024.

[5] A. Waleed et al., “Lead-Free Perovskite Nanowire Array Photodetectors with Drastically Improved Stability in Nanoengineering Templates”, vol. 17, no. 1, pp. 523–530, Dec. 2016.

[6] Z. Long, Y. Ding, X. Qiu, Y. Zhou, S. Kumar, and Z. Fan, “A dual-mode image sensor using an all-inorganic perovskite nanowire array for standard and neuromorphic imaging”, Journal of Semiconductors, vol. 44, no. 9, p. 092604, Sep. 2023.

[7] L. Gu et al., “A biomimetic eye with a hemispherical perovskite nanowire array retina”, Nature, vol. 581, no. 7808, pp. 278–282, May 2020.

[8] L. Gu et al., “3D Arrays of 1024-Pixel Image Sensors based on Lead Halide Perovskite Nanowires”, Advanced Materials, vol. 28, no. 44, pp. 9713–9721, Sep. 2016.

[9] S. Poddar et al., “Down-Scalable and Ultra-fast Memristors with Ultra-high Density Three-Dimensional Arrays of Perovskite Quantum Wires”, Nano Letters, vol. 21, no. 12, pp. 5036–5044, Jun. 2021.